Article

Effect of Explicit Cationic Size and Valence Constraints on the Phase Stability of 1:2 B-Site-Ordered Perovskite Ruthenates

Job T. Rijssenbeek, Takashi Saito, Sylvie Malo, Masaki Azuma, Mikio Takano, and Kenneth R. Poeppelmeier

J. Am. Chem. Soc., **2005**, 127 (2), 675-681• DOI: 10.1021/ja044797w • Publication Date (Web): 18 December 2004

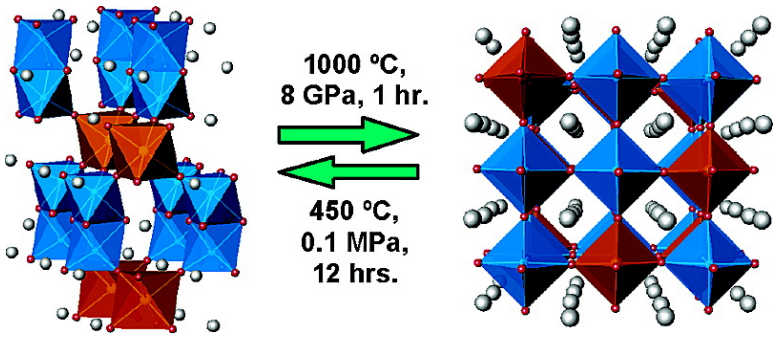

More About This Article

Additional resources and features associated with this article are available within the HTML version:

- Supporting Information
- Links to the 2 articles that cite this article, as of the time of this article download
- Access to high resolution figures
- Links to articles and content related to this article
- Copyright permission to reproduce figures and/or text from this article

View the Full Text HTML

J|A|C|S
ARTICLES
Published on Web 12/18/2004

Effect of Explicit Cationic Size and Valence Constraints on the Phase Stability of 1:2 B-Site-Ordered Perovskite Ruthenates

Job T. Rijssenbeek,[†,#] Takashi Saito,[‡] Sylvie Malo,[§] Masaki Azuma,[‡] Mikio Takano,[‡] and Kenneth R. Poeppelmeier*[,†]

Contribution from the Department of Chemistry, Northwestern University, Evanston, Illinois 60208-3113, Institute for Chemical Research, Kyoto University, Uji, Kyoto-fu 611, Japan, and Laboratoire CRISMAT-ENSICAEN, Université de Caen, 6 Boulevard du Maréchal Juin, 14050 Caen, Cedex, France

Received August 28, 2004; E-mail: krp@northwestern.edu

Abstract: The related parameters of cation size and valence that control the crystallization of $Sr_3CaRu_2O_9$ into a 1:2 B-site-ordered perovskite structure were explored by cationic substitution at the strontium and calcium sites and by the application of high pressure. At ambient pressures, $Sr_3MRu_2O_9$ stoichiometries yield multiphasic mixtures for M = Ni^{2+}, Mg^{2+}, and Y^{3+}, whereas pseudocubic perovskites result for M = Cu^{2+} and Zn^{2+}. For A-site substitutions, an ordered perovskite structure results for $Sr_{3-x}Ca_xCaRu_2O_9$, with $0 \le x \le 1.5$. In contrast, Ba^{2+} substitution for Sr^{2+} is accompanied by a phase change to a hexagonal $BaTiO_3$ structure type. At high pressures and temperatures, a 1:2 B-site-ordered perovskite structure is stabilized for $Sr_{3-x}Ba_xCaRu_2O_9$, with $0 \le x \le 3$. The scarcity of B-site-ordered perovskite ruthenates at ambient pressure and the metastable nature of the high-pressure phases underscore the strict size and valence requirements that must be met by the constituent cations to achieve these uncommon ordered structures.

1. Introduction

The varied chemistry of ruthenium-based oxides results in a host of fascinating physical properties, such as itinerant ferromagnetism in $SrRuO_3$[1] and unconventional superconductivity in Sr_2RuO_4.[2] Combining ruthenium with other metals in an ordered fashion within a perovskite (ABO_3) framework can lead to even more exotic properties, such as the coexistence of magnetism and superconductivity, as in the layered $RuSr_2GdCu_2O_8$ (Ru-1212).[3] Our studies of cation-ordered mixed-metal ruthenates, such as Ru-1212, led us to the unexpected discovery of $Sr_3CaRu_2O_9$,[4] which crystallizes with a 1:2 B-site-ordered perovskite structure (Figure 1). The 1:2 B-site ordering was heretofore unknown for transition metals with partially filled d-orbitals (Ru^{5+}: t^3e^0) and prompted us to investigate other related perovskite ruthenates to understand the factors that stabilize the cation ordering.

We have pursued two approaches to investigate the B-site cation ordering in $Sr_3CaRu_2O_9$. First, we explored isovalent and heterovalent substitution at both the strontium and calcium positions. Second, we performed syntheses under high pressures to favor the formation of perovskite structures for compositions like $Ba_3CaRu_2O_9$, which crystallize with the 6H hexagonal barium titanate structure at ambient pressure (Figure 2).[5] The 6H structure type is common for the $Ba_3MRu_2O_9$ family of compounds wherein M is almost any di- or trivalent cation[6−8] as well as several mono-[9] and tetravalent[10,11] cations. Several

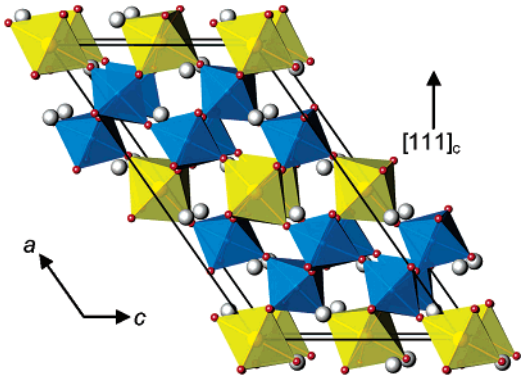

Figure 1. Unit cell of $Sr_3CaRu_2O_9$ viewed along the [010] direction. Yellow octahedra are CaO_6, and blue octahedra are RuO_6. The cubic [111] direction is vertical on the page.

[†] Northwestern University.
[‡] Kyoto University.
[§] Université de Caen.
[#] Current address: GE Global Research, One Research Circle, Niskayuna, NY 12309.

(1) Callaghan, A.; Moeller, C. W.; Ward, R. *Inorg. Chem.* **1966**, *5*, 1572.
(2) Maeno, Y.; Hashimoto, H.; Yoshida, K.; Nishizaki, S.; Fujita, T.; Bednorz, J. G.; Lichtenberg, F. *Nature* **1994**, *372*, 532.
(3) Bauernfeind, L.; Widder, W.; Braun, H. F. *Physica C* **1995**, *254*, 151−158.
(4) Rijssenbeek, J. T.; Malo, S.; Caignaert, V.; Poeppelmeier, K. R. *J. Am. Chem. Soc.* **2002**, *124*, 2090−2091.
(5) Darriet, J.; Drillon, M.; Villeneuve, G.; Hagenmuller, P. *J. Solid State Chem.* **1976**, *19*, 213−220.
(6) Donohue, P. C.; Katz, L.; Ward, R. *Inorg. Chem.* **1966**, *5*, 339−342.
(7) Rijssenbeek, J. T.; Huang, Q.; Erwin, R. W.; Zandbergen, H. W.; Cava, R. J. *J. Solid State Chem.* **1999**, *146*, 65.
(8) Doi, Y.; Matsuhira, K.; Hinatsu, Y. *J. Solid State Chem.* **2002**, *165*, 317.
(9) Stitzer, K. E.; Smith, M. D.; Gemmill, W. R.; zur Loye, H.-C. *J. Am. Chem. Soc.* **2002**, *124*, 13877−13885.
(10) Müller-Buschbaum, H.; Mertens, B. *Z. Naturforsch., B* **1996**, *51*, 79−84.

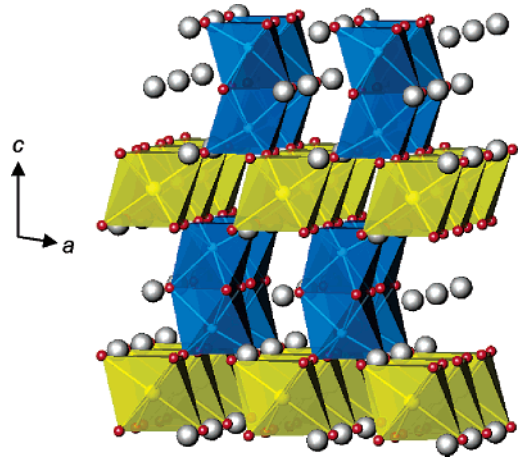

Figure 2. The 6H hexagonal barium titanate structure adopted by many $Ba_3MRu_2O_9$ compounds. RuO_6 octahedra are blue, and MO_6 octahedra are yellow.

literature reports indicate that these hexagonal perovskite polytypes can be transformed to cubic perovskite structures by cationic substitution and/or the application of pressure.[12,13] The application of pressure or the reduction of the average A-cation radius by substitution favors a greater degree of cubic stacking (i.e., corner-sharing octahedra), which suggests that the 6H structure of $Ba_3CaRu_2O_9$ might, under applied pressure, adopt a perovskite structure like that of $Sr_3CaRu2O_9$.

2. Experimental Section

To examine substitution on the calcium site (B-site), samples with compositions of $Sr_3MRu_2O_9$ (M = Ni, Mg, Cu, Zn, and Y) were prepared via solid-state reaction of stoichiometric amounts of $SrCO_3$, MO or $MO_{1.5}$, and RuO_2. The reagents were ground in an agate mortar and calcined in alumina crucibles overnight at 850 °C. The samples were then reground, pressed into pellets, and fired at 1200 °C in 1 atm of flowing oxygen for 48 h with one intermediate regrinding. The B-site-substituted samples were treated in a high-pressure oxygen furnace (Morris Research Inc.) up to 320 atm at 1000 °C to minimize oxygen vacancies and promote pentavalent ruthenium.

To elucidate the effect of substitution on the strontium site (A-site), samples of $Sr_{3-x}A_xCaRu_2O_9$ ($0 \le x \le 3$; A = Ca^{2+} or Ba^{2+}) were prepared as above from $SrCO_3$, ACO_3, and RuO_2. Concurrent substitution at both A- and B-sites was investigated by synthesis of $Ba_3MRu_2O_9$ with M = Ni,[14] Cu,[7] and Y[15] from $BaCO_3$, RuO_2, and NiO, CuO, and $YO_{1.5}$, respectively. All reagents were each at least 99.95% pure.

High-pressure (HP) samples of $Sr_{3-x}Ba_xCaRu_2O_9$ ($0 \le x \le 3$) and $Ba_3MRu_2O_9$ (M = Ni, Cu, and Y) were synthesized from the ambient pressure (AP) precursors of the same stoichiometry (see above). Approximately 150 mg of powder was packed in a gold capsule and subjected to an applied pressure of 8 GPa in a cubic anvil press for 1 h at up to 1400 °C.

Powder X-ray diffraction (PXD) was used for phase identification. Diffraction patterns were recorded with a Rigaku XDS 2000 diffractometer using nickel-filtered Cu Kα radiation (λ = 1.5418 Å) over a range of $10° < 2\theta < 80°$ in 0.05° steps with a 1 s counting time per step. Electron diffraction (ED) studies were performed on several crystallites of each sample using a JEOL 200CX electron microscope fitted with a eucentric goniometer (±60°). Samples were prepared by dispersing crystallites on a holey carbon film supported by a copper grid. Energy-dispersive X-ray spectroscopy (EDS) analysis was performed, using the same microscope, on multiple crystallites to verify the cationic composition of the calcium-substituted samples. For HP $Ba_3CaRu_2O_9$, time-of-flight neutron diffraction data were collected on approximately 350 mg (from three HP runs) of powder using the special environment powder diffractometer at the Intense Pulsed Neutron Source at Argonne National Laboratory. The structural model for HP $Ba_3CaRu_2O_9$ was refined based on the neutron data from the high-resolution backscatter bank ($\Delta d/d = 0.0035$) using the Rietveld method in the General Structure Analysis System (GSAS) refinement package.[16]

3. Results and Discussion

Cationic substitutions on both the strontium and the calcium sites probe the factors that control the crystallization of $Sr_3CaRu_2O_9$ into a 1:2 B-site-ordered perovskite structure. On the strontium site ($r_{Sr^{2+}}$ = 1.44 Å; atomic radii compiled by Shannon[17]), substitutions with calcium ($r_{Ca^{2+}}$ = 1.34 Å) and barium ($r_{Ba^{2+}}$ = 1.61 Å) were performed to study the effect of the A-site on the phase stability. To investigate the effects of the minority B-site Ca^{2+} ($r_{Ca^{2+}}$ = 1.00 Å) on the structure, syntheses of the form $Sr_3MRu_2O_9$ were attempted for M = Ni^{2+} ($r_{Ni^{2+}}$ = 0.69 Å), Mg^{2+} ($r_{Mg^{2+}}$ = 0.72 Å), Cu^{2+} ($r_{Cu^{2+}}$ = 0.73 Å), and Zn^{2+} ($r_{Zn^{2+}}$ = 0.74 Å). Heterovalent doping with Y^{3+} ($r_{Y^{3+}}$ = 0.90 Å) for Ca^{2+} was performed to create Ru^{4+}/Ru^{5+} mixed valency and thereby induce an insulator to metal transition.

3.1. Substitution for Calcium at Ambient Pressure. None of the substitutions on the calcium site ($Sr_3MRu_2O_9$ where M = Ni^{2+}, Mg^{2+}, Cu^{2+}, and Zn^{2+}) yielded a 1:2-ordered perovskite structure, likely because the substituting cations are all appreciably smaller than calcium. For Ni^{2+} and Mg^{2+}, the smallest cations, the result was a mixture of Sr_2RuO_4, $SrRuO_3$, and MO (M = Ni^{2+} or Mg^{2+}; Figure 3a,b). Even syntheses under 320 bar of oxygen at 900 °C did not promote a pentavalent ruthenate that incorporated the magnesium or nickel. For the larger Cu^{2+} and Zn^{2+} (Figure 3c,d), a monophasic pseudocubic perovskite was formed; however, the absence of superlattice reflections indicated that the Cu^{2+} (or Zn^{2+}) and Ru^{5+} cations were randomly distributed over the perovskite B-sites. For these latter substitutions, although a perovskite structure was formed, the charge and/or ionic size difference with Ru^{5+} was insufficient to segregate the cations onto distinct sites. To more accurately reflect the structure, the formula could be written $Sr(M_{1/3}Ru_{2/3})O_3$ (M = Cu^{2+} or Zn^{2+}). These substitution patterns are consistent with those of a study of $Ca(Ru_{1-x}M_x)O_3$ (M = Ni^{2+}, Cu^{2+}, and Zn^{2+}) in which relatively large solubilities were found for Cu^{2+} (x = 0.1) and Zn^{2+} (x = 0.25), while a limit of only x = 0.05 was established for Ni^{2+}.[18] That isovalent substitutions of calcium failed to yield a 1:2-ordered perovskite structure illustrates the critical role of the calcium ion's size in stabilizing $Sr_3CaRu_2O_9$. In the unique case of M = Ca^{2+}, the radius of Ca^{2+} is small enough to occupy the six-coordinate perovskite B-site yet large enough to simultaneously foster cation ordering.

The absence of cation ordering between Cu^{2+} and Ru^{5+} is particularly surprising. On the basis of the traditional arguments of size, charge, and coordination preference, copper and ruthenium appear to be ideal candidates to form cation-ordered

(11) Doi, Y.; Wakeshima, M.; Hinatsu, Y.; Tobo, A.; Ohoyama, K.; Yamaguchi, Y. *J. Mater. Chem.* **2001**, *11*, 3135−3140.
(12) Longo, J. M.; Kafalas, J. A. *Mater. Res. Bull.* **1968**, *3*, 687.
(13) Battle, P. D.; Jones, C. W.; Lightfoot, P.; Strange, R. *J. Solid State Chem.* **1990**, *85*, 144.
(14) Lightfoot, P.; Battle, P. D. *J. Solid State Chem.* **1990**, *89*, 174.
(15) Treiber, U.; Kemmler-Sack, S.; Ehmann, A.; Schaller, H. U.; Duerrschmidt, E.; Thumm, I.; Bader, H. *Z. Anorg. Allg. Chem.* **1981**, *481*, 143.
(16) Larson, A. C.; Von Dreele, R. B. Los Alamos National Laboratory, [Rep.] LANL **1994**, LAUR 86−748.
(17) Shannon, R. D. *Acta Crystallogr.* **1976**, *A32*, 751.
(18) He, T.; Cava, R. J. *J. Phys.: Condens. Matter* **2001**, *13*, 8347−8361.

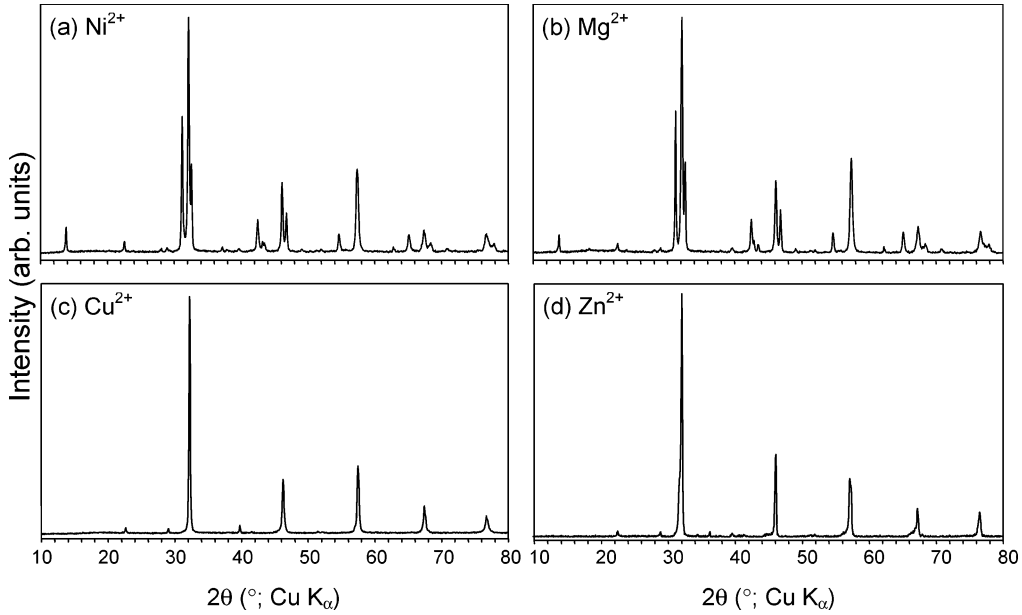

Figure 3. Powder X-ray diffraction patterns of preparations of $Sr_3MRu_2O_9$, M = Ni^{2+}, Mg^{2+}, Cu^{2+}, and Zn^{2+}. For M = Ni^{2+} (a) and Mg^{2+} (b), a mixture of Sr_2RuO_4, $SrRuO_3$, and MO results. For M = Cu^{2+} (c) and Zn^{2+} (d), a single-phase pseudocubic perovskite is formed.

perovskites. In octahedral coordination, the difference in their tabulated ionic radii,[17] $\Delta r = 0.165$ Å, is larger than all but one known randomly ordered perovskite ($CaBaZrGeO_6$; $\Delta r = 0.190$ Å).[19] The charge difference is also large: three for Cu^{2+} and Ru^{5+}. The differences in coordination preferences are similarly large owing to the Jahn−Teller distortion of $Cu^{2+}(3d^9)$, which favors tetragonally distorted octahedral environments. Yet despite these differentiating factors, no order was found in $Sr(Cu_{1/3}Ru_{2/3})O_3$, and literature examples of ordered copper−ruthenium perovskites are extremely rare. Excluding oxygen-deficient structures, only $LaBaCu^{2+}Ru^{5+}O_6$ (rock-salt) and $La_2Cu^{2+}Ru^{4+}O_6$ have been reported to adopt ordered structures. In fact, the ordering in the latter is only partial and rather tenuous. One octahedral site contains ~80% Cu and ~20% Ru, with the inverse distribution on the other site, and substitution of 20% of the Ru^{4+} with Ti^{4+} yields a pseudocubic structure.[21]

Full substitution of Y^{3+} for Ca^{2+} on the B-site yielded a mixture of Sr_2YRuO_6 and $SrRuO_3$ (Figure 4). Preparations with partial substitution were composed of a mixture of Sr_2YRuO_6, $SrRuO_3$, and $Sr_3CaRu_2O_9$. The amounts of $SrRuO_3$ and Sr_2YRuO_6 increased with increasing yttrium content, while no changes in the peak positions of the 1:2-ordered phase were detected, indicating that no appreciable substitution of Y^{3+} for Ca^{2+} had taken place.

3.2. Substitution for Strontium at Ambient Pressure. The solubility range of Ca^{2+} on the A-site, as determined by PXD, extends to approximately 50% substitution (i.e., $(Sr_{3-x}Ca_x)CaRu_2O_9$, $0 \le x \le 1.5$; Figure 5). The shift in peak positions toward higher 2θ is consistent with a smooth decrease in the lattice parameters as the smaller calcium substitutes for the strontium. For $x > 1.5$, the 1:2-ordered perovskite is no longer stable, and multiphasic products are favored. EDS analysis of the nominally $x = 1.0$ sample determined the cation ratios to be $Sr_{2.35}Ca_{1.73}Ru_{2.0}$ (normalized to ruthenium), which confirms the substitution of calcium for strontium, albeit, at levels lower than expected. For the fully substituted stoichiometry, $CaRuO_3$ and CaO (in an equimolar ratio) are the only products. The $CaRuO_3$ could not be oxidized by treatment under 320 atm of oxygen at 1000 °C to favor a single phase with pentavalent ruthenium. From these results, a lower limit of approximately 1.39 Å is established for the average radius of the A-site. This

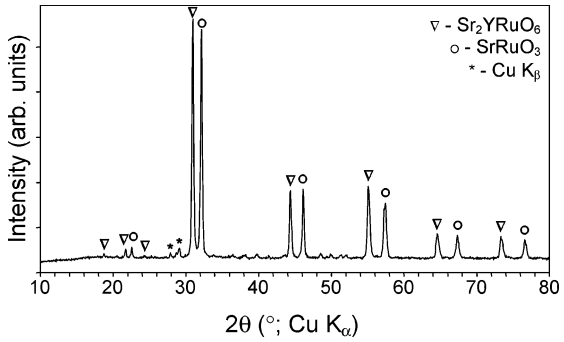

Figure 4. Powder X-ray diffraction patterns of $Sr_3YRu_2O_9$, which is a mixture of Sr_2YRuO_6 (▽) and SrRuO3 (○). The ∗ denotes the peaks resulting from K_β radiation.

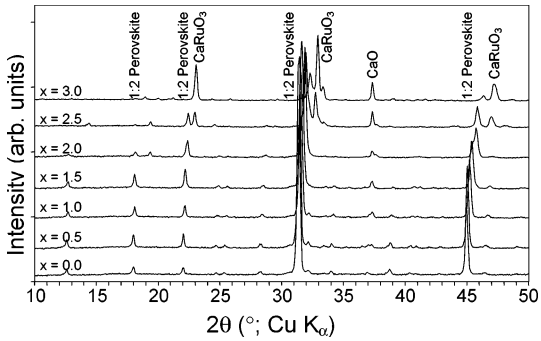

Figure 5. Powder X-ray diffraction patterns of $(Sr_{3-x}Ca_x)CaRu_2O_9$ for $0 \le x \le 3$. The 1:2-ordered perovskite is stable for $0 \le x \le 1.5$. For $x = 3$, $CaRuO_3$ and CaO are the only products.

(19) Anderson, M. T.; Greenwood, K. B.; Taylor, G. A.; Poeppelmeier, K. R. *Prog. Solid State Chem.* **1993**, *22*, 197.
(20) Rozier, P.; Jansson, K.; Nygren, M. *Mater. Res. Bull.* **2000**, *35*, 1391−1400.
(21) Battle, P. D.; Frost, J. R.; Kim, S.-H. *J. Mater. Chem.* **1995**, *5*, 1003−1006.

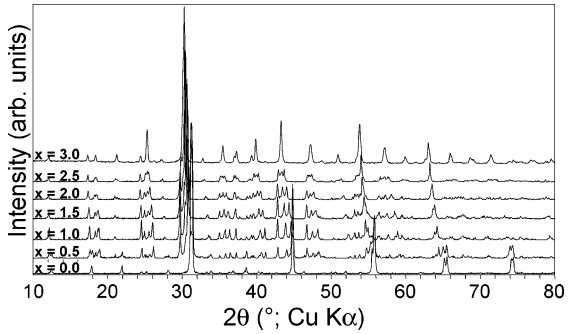

Figure 6. Powder X-ray diffraction patterns of the series $Sr_{3-x}Ba_xCaRu_2O_9$, $0 \le x \le 3$.

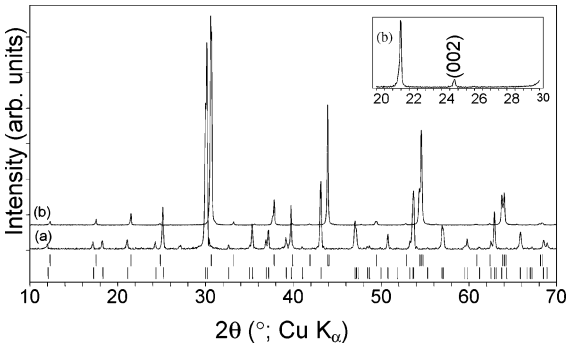

Figure 7. (a) Powder X-ray diffraction pattern of ambient pressure for $Ba_3CaRu_2O_9$. Bragg reflections (lower bars) are based on a hexagonal $P6_3/mmc$ unit cell with $a = b = 5.891$ Å and $c = 14.571$ Å. (b) Diffraction profile of high-pressure $Ba_3CaRu_2O_9$. Bragg reflections (upper bars) are based on a hexagonal $P\bar{3}m1$ unit cell with $a = b = 5.8168(2)$ Å and $c = 7.1619(3)$ Å. Inset: enlargement of the $20° \le 2\theta \le 30°$ region of pattern (b). The single peak at 24.7° indicates that there is no octahedral tilting.

contrasts sharply with the niobium-based series $Sr_{3-x}Ca_x$-$CaNb_2O_9$, which forms a 1:2-ordered perovskite for all values of x.[22,23]

Substitution of the larger barium for strontium, $Sr_{3-x}Ba_x$-$CaRu_2O_9$, resulted in a mixture of the 1:2-ordered perovskite and a hexagonal $BaTiO_3$-type perovskite polytype[5] for $x \le 0.5$ (Figure 6). For larger values of x, the hexagonal perovskite polytype was the only product, indicating that there is no appreciable solubility of barium on the strontium site in the perovskite structure of $Sr_3CaRu_2O_9$. This suggests that the maximum average A-site radius for the perovskite structure is approximately 1.44 Å. However, the significant tilting of the RuO_6 octahedra in $Sr_3CaRu_2O_9$ suggests that, structurally, it must be possible to accommodate larger A-cations.[4] Therefore, the fact that the perovskite structure forms only for the fully strontium-substituted composition is linked to the great stability of the 6H phase and not to an instability of the ordered perovskite structure.

3.3. Substitution for Strontium at High Pressure. The application of pressure is an ideal way to destabilize the 6H structure in favor of a higher-density perovskite arrangement. After an hour-long treatment at 8 GPa and 1000 °C, the diffraction pattern of HP $Ba_3CaRu_2O_9$ (Figure 7) is drastically different from that of the AP phase and is clearly reminiscent of a 1:2-ordered perovskite structure related to $Ba_3ZnTa_2O_9$.[24]

Table 1. Neutron Refinement Parameters for High-Pressure $Ba_3CaRu_2O_9$

formula	$Ba_3CaRu_2O_9$
space group	$P\bar{3}m1$ (#164)
a (Å)	5.8168(2)
b (Å)	5.8168(2)
c (Å)	7.1619(3)
V (Å^3)	209.86(2)
Z	1
radiation	time-of-flight neutron[a]
d range (Å)	0.48−3.94
refinement software	GSAS[b]
R_p	4.97%
R_{wp}	7.96%
χ^2	1.49
reflections	817
parameters	30

[a] SEPD at IPNS at Argonne National Laboratory. [b] See ref 16.

Table 2. Refined Atomic Positions and Isotropic Thermal Parameters for High-Pressure $Ba_3CaRu_2O_9$

atom	Wyckoff	x	y	z	B_{iso}[a]
Ba1	1a	0	0	0	0.59(12)
Ba2	2d	1/3	2/3	0.6713(8)	0.75(7)
Ca	1b	0	0	1/2	0.89(15)
Ru	2d	1/3	2/3	0.1616(5)	0.39(5)
O1	3e	1/2	0	0	1.15(7)
O2	6i	0.1781(2)	−0.1781(2)	0.3146(3)	0.99(5)

[a] All sites were assumed to be fully occupied.

Table 3. Selected Interatomic Distances in High-Pressure $Ba_3CaRu_2O_9$

bond	distance (Å)
Ba1−O1	2.892(5) × 3
Ba1−O2	2.996(4) × 3
Ba1−O2	2.9124(3) × 6
Ba2−O1	2.9084(1) × 6
Ba2−O2	2.880(2) × 6
Ca−O2	2.232(2) × 6
Ru−O1	2.040(2) × 3
Ru−O2	1.910(3) × 3

The presence of a single peak (the 002 reflection) in the $24° < 2\theta < 26°$ range (Figure 7, inset) is characteristic of a structure with untilted octahedra (e.g., $Sr_3CaRu_2O_9$, with tilted octahedra, has two peaks in this range).[25] The relative insensitivity of X-rays to the oxide positions prevents slight octahedral rotations or tilts from being ruled out on the basis of PXD alone. The ED patterns (Figure 8) showed only reflections attributable to a trigonal unit cell with $a = b \approx 5.8$ Å and $c \approx 7.1$ Å. The extinction conditions were consistent with space group $P\bar{3}m1$, which is expected for a 1:2 B-site-ordered structure with untilted BO_6 octahedra.[26] Electron diffraction is particularly sensitive to superstructural features; therefore, the fact that no supercell reflections were observed is strong evidence that there is no tilting of the RuO_6 octahedra.

The crystal structure of $Ba_3CaRu_2O_9$ was refined based on the ToF neutron diffraction data in space group $P\bar{3}m1$ (#164), using $Ba_3ZnTa_2O_9$ as the initial model[24] (Figure 9). All sites were assumed to be fully occupied, and the thermal parameters were grouped by atom type and refined together. The final

(22) Hervieu, M.; Studer, F.; Raveau, B. *J. Solid State Chem.* **1977**, *22*, 273−289.
(23) Hervieu, M.; Raveau, B. *J. Solid State Chem.* **1979**, *28*, 209−222.
(24) Jacobson, A. J.; Collins, B. M.; Fender, B. E. F. *Acta Crystallogr.* **1982**, *B24*, 1968.
(25) Rijssenbeek, J. T.; Malo, S.; Saito, T.; Caignaert, V.; Azuma, M.; Takano, M.; Poeppelmeier, K. R. *Perovskite Materials*. MRS Proceedings, 2002; Vol. 718, p 3.
(26) Levin, I.; Bendersky, L. A.; Cline, J. P.; Roth, R. S.; Vanderah, T. A. *J. Solid State Chem.* **2000**, *150*, 43.

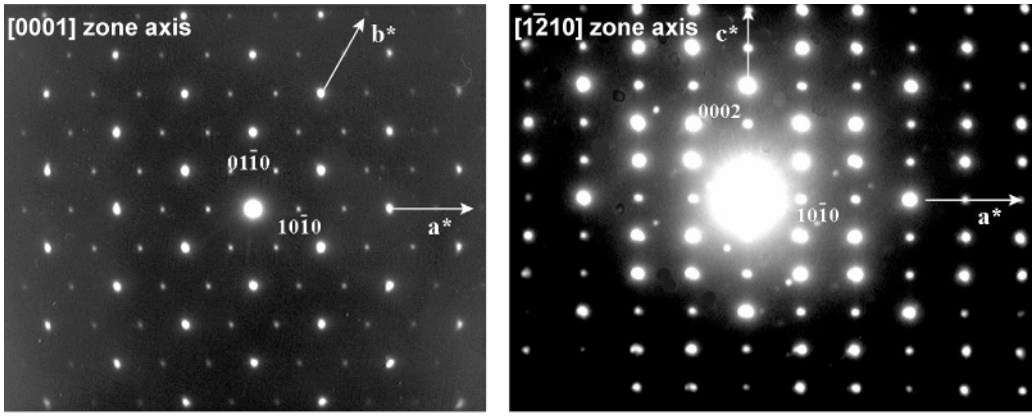

Figure 8. Electron diffraction patterns of HP $Ba_3CaRu_2O_9$ taken along the (a) [0001] and (b) [1-210] zone axes.

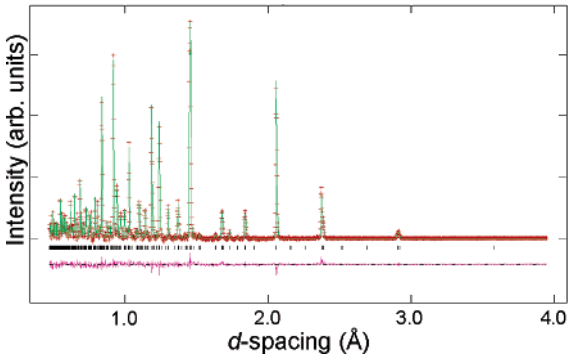

Figure 9. Rietveld refined time-of-flight powder neutron diffraction profile of HP $Ba_3CaRu_2O_9$ (backscatter detector bank at 144.85°). Data (red crosses), fitted profile (green line), allowed Bragg reflections (black bars), and difference curve (purple lower line) are shown.

refinement cycle yielded lattice parameters $a = b = 5.8168(2)$ Å ($\approx\sqrt{2}a_p$), $c = 7.1619(3)$ Å ($\approx\sqrt{3}a_p$) and $Z = 1$, and $R_p = 4.97\%$, $R_{wp} = 7.96\%$, and $\chi^2 = 1.49$. Relevant details regarding the data collection and refinement are given in Table 1. Selected atomic coordinates, isotropic thermal parameters, and interatomic distances are given in Tables 2 and 3.

The structure is that of a 1:2-ordered perovskite with no tilting of the $(Ca/Ru)O_6$ octahedra. As such, HP $Ba_3CaRu_2O_9$ represents only the second example of this structure type with a non-d^0 majority metal. The Ca^{2+} and Ru^{5+} are sequenced {...−Ca−Ru−Ru−...} in the direction both perpendicular to the close packed planes (Figure 10a) and along each of the three pseudocubic directions in perovskite (Figure 10b). The large barium can be accommodated on the 12-coordinate A-site without tilting of the $(Ca/Ru)O_6$ octahedra. However, the average Ca−O (2.232 Å) and Ru−O (1.975 Å) bond lengths are appreciably different from each other, reflecting the disparity in their ionic radii. As those in $Sr_3CaRu_2O_9$, the Ca−O bonds are slightly compressed ($Ca-O_{expected} \approx 2.4$ Å), while the average Ru−O bond ($Ru-O_{expected} \approx 1.965$ Å) is close to that expected from the sum of the ionic radii. Consistent with the symmetry of the space group, there is significant anisotropy in the bond lengths around the ruthenium, which is shifted toward one face of its octahedron. Normally, this would be unfavorable for a metal with partially filled d-orbitals, but the high degree of covalency of the Ru−O bonds likely mitigates the negative electron−electron interactions. The transformation of the AP hexagonal perovskite polytype to the ordered perovskite is accompanied by a ~5% reduction in volume, which corresponds to a stabilization energy of approximately 40 kJ/mol at 6 GPa. The conversion can be achieved for all members of the $Sr_{3-x}Ba_xCaRu_2O_9$ series and can be reversed by heating at 450 °C at ambient pressure. It should be noted here that subjecting $Sr_3CaRu_2O_9$ to high pressures did not change the crystal structure nor the cation ordering.

3.4. Substitution on Both A- and B-Sites at High Pressure. We anticipated that the transformation of 6H $Ba_3CaRu_2O_9$ to

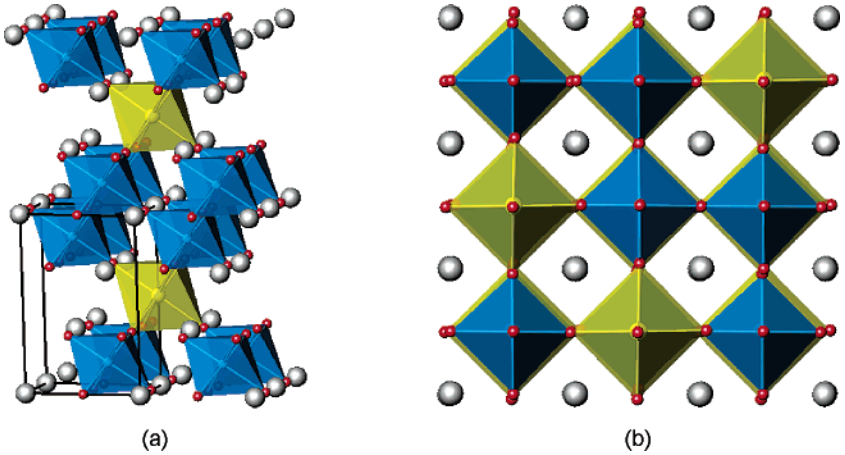

Figure 10. Structure of HP $Ba_3CaRu_2O_9$ (a) viewed along the close-packed planes and (b) viewed along one of the pseudocubic directions of perovskite. CaO_6 octahedra are yellow, and RuO_6 octahedra are blue.

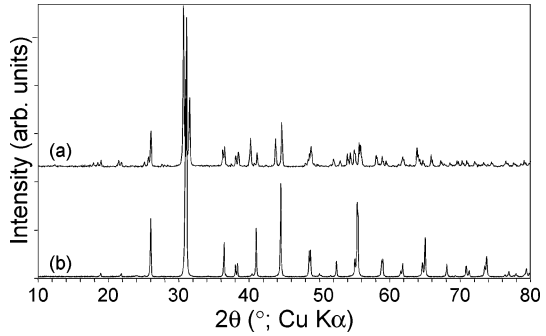

Figure 11. Powder X-ray diffraction profiles of (a) ambient pressure and (b) high-pressure $Ba_3Cu_2O_9$. Note the orthorhombic splitting of the main peaks in the AP pattern is much reduced in the higher symmetry HP pattern.

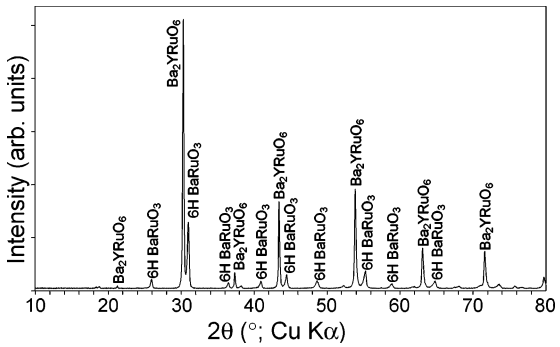

Figure 12. Powder X-ray diffraction profile of Ba_3YRu2O_9 treated at 1200 °C under 8 GPa for 1 h. The main peaks attributed to Ba_2YRuO_6 and 6H $BaRuO_3$ are labeled.

perovskite under pressure might lead to the discovery of other ordered mixed-metal perovskite ruthenates. Because the 6H structure is ubiquitous in the Ba−M−Ru−O system, the investigation of possible transformations was likely to be fruitful. Specifically, we investigated $Ba_3MRu_2O_9$ with M = Ni,[14] Cu[7], and Y[15] to determine the phase stability of HP $Ba_3CaRu_2O_9$ and whether other ordered perovskites were accessible.

For $Ba_3NiRu_2O_9$, no change in the PXD pattern was detected after high-pressure treatment, which indicates that a 1:2-ordered nickel−ruthenium perovskite is not stable up to 8 GPa. This is consistent with the finding that $Sr_3NiRu_2O_9$ also does not form a B-site-ordered structure. On the other hand, the PXD pattern of HP $Ba_3CuRu_2O_9$ heated to 1400 °C under 8 GPa for 30 min was notably different from the AP pattern (Figure 11). However, the HP structure is not perovskite-like but retains the 6H-type structure, although the applied pressure induced a disordering of the Cu^{2+} and Ru^{5+} over all B-sites, yielding a higher symmetry structure. It is likely that higher pressures would stabilize a perovskite structure, although Cu/Ru ordering seems unlikely given the disordered nature of $Sr(Cu_{1/3}Ru_{2/3})O_3$.

$Ba_3YRu_2O_9$ was synthesized to yield a mixed-valence ruthenate (Ru^{4+}/Ru^{5+}) that might be transformed by the action of high pressure. This mixed valence is stable at ambient pressure in the 6H structure;[8] however, treatment at high pressure did not result in a 1:2-ordered perovskite. After it was heated at 1200 °C under 8 GPa for 1 h, the PXD profile (Figure 12) revealed an equimolar mixture of Ba_2YRuO_6 and 6H $BaRuO_3$. The former is a 1:1 B-site-ordered perovskite with Y^{3+} and Ru^{5+},[27] while the latter is the stable polytype of $BaRuO_3$ at 8 GPa and contains only Ru^{4+}.[12]

The results presented in this paper are summarized in Figure 13, which illustrates the factors that govern the formation of $Sr_3CaRu_2O_9$ and HP $Ba_3CaRu_2O_9$. The fact that only compositions with Ca and Ru on the B-site form the 1:2 B-site-ordered perovskite structures is quite surprising and highlights the confluence of several geometric and stoichiometric requirements that are only satisfied by a very limited number of constituent elements. In both $Sr_3CaRu_2O_9$ and HP $Ba_3CaRu_2O_9$, the particular choice of constituent elements makes possible a perovskite structure as opposed to other conceivable alternatives. That calcium ($r_{Ca^{2+}} = 1.00$ Å) is one of the largest cations that can be accommodated on the octahedral B-site of perovskite is crucial because smaller divalent cations (e.g., Ni^{2+}, Mg^{2+}, Cu^{2+}, or Zn^{2+}) do not form ordered perovskites when combined with Ru^{5+} ($r_{Ru^{5+}} = 0.565$ Å). In fact, only the largest two (Cu^{2+} and Zn^{2+}) form a mixed-metal perovskite structure. Cations larger than calcium (e.g., Sr^{2+}) do not fit into the octahedral sites of the perovskite structure (at least, when Sr^{2+} is the A-cation), and therefore yield polytype structures, such as $Sr_4Ru_2O_9$[28], or multiphasic products.

Under pressure, the area of perovskite stability in Figure 13 is extended to include compositions with larger average A-cation radii. The large size of calcium allows the tolerance factor of $Ba_3CaRu_2O_9$ to remain small enough ($t = 1.009$), such that

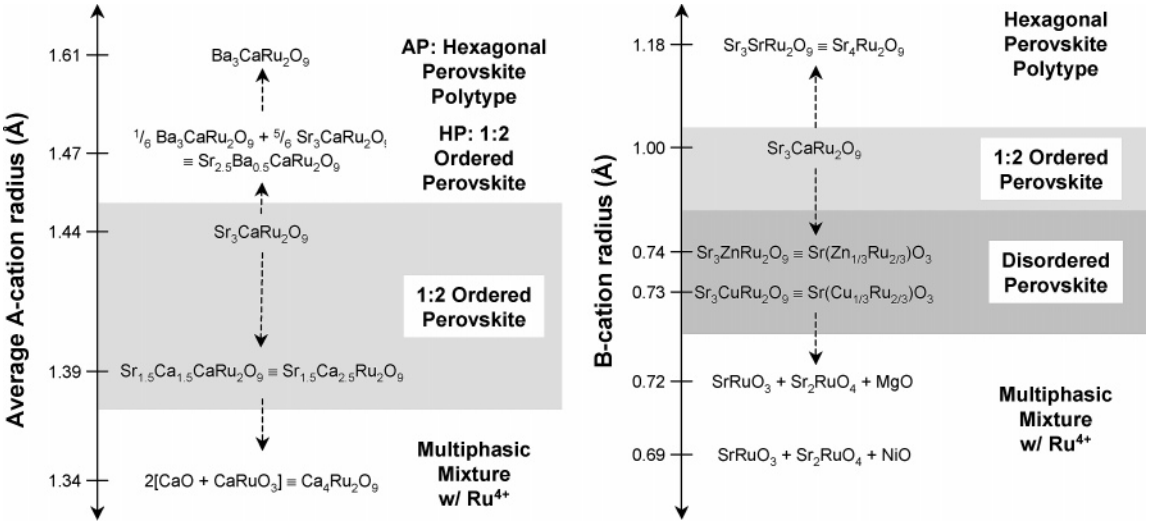

Figure 13. Summary of structures and compositions formed in the $A_3BRu_2O_9$ system as a function of isovalent A- and B-cation sizes.

under pressure, the perovskite structure is preferred over a hexagonal polytype structure. The tolerance factors of $Ba_3NiRu_2O_9$ ($t = 1.061$) and $Ba_3CuRu_2O_9$ ($t = 1.054$) are appreciably larger than unity; therefore, these compounds retain the 6H structure even under pressure. On the basis of the size arguments described above, Y^{3+} ($r_{Y^{3+}} = 0.900$ Å; $t = 1.016$) might be expected to take a perovskite structure under pressure. In fact, a perovskite does result (Ba_2YRuO_6); however, this is at a 1:1 stoichiometry, leaving behind $BaRuO_3$. $Ba_3CaRu_2O_9$ cannot disproportionate in the same fashion because Ba_2CaRuO_6 would require highly oxidized Ru^{6+}, which cannot be achieved under the synthetic conditions of our experiments. Thus, $Ba_3CaRu_2O_9$ exhibits a unique combination of factors that allows the transformation of the hexagonal polytype to the 1:2 B-site-ordered perovskite structure by the application of high pressure.

In addition to the essential role of calcium, the A-site cation is similarly important in stabilizing the perovskite structure. At ambient pressure, the formation of perovskite with even small amounts of barium is defeated by the exceptional stability of the 6H structure for mixed-metal ruthenates with barium. Thus the 1:2 B-site-ordered structure forms only when the average A-cation radius is less than or equal to that of strontium ($r_{Sr^{2+}} = 1.44$ Å). Reducing the average A-site cation size by substituting more than one-half of the Sr^{2+} by Ca^{2+} results in multiphasic mixtures wherein the cation stoichiometry is accommodated by reduction of the ruthenium. The perovskite structure is stable only when the size of the A-site cation falls in the range of $1.39 \text{ Å} \leq r_{A-site} \leq 1.44$ Å (Figure 13). Both the upper and lower limits are determined by the small ionic radius of ruthenium ($r_{Ru^{5+}} = 0.565$ Å) because niobium-based 1:2-ordered perovskites ($r_{Nb^{5+}} = 0.64$ Å) are known outside of this A-cation size range (e.g., $Ca_3CaNb_2O_9$ and $Ba_3CaNb_2O_9$).[5,29] In addition to the average size, the disparity of the sizes can be expected to have an effect on the resulting structure, as it does in manganates and cuprates.[30]

4. Conclusion

$Sr_3CaRu_2O_9$ and HP $Ba_3CaRu_2O_9$ are the only examples of 1:2 B-site-ordered perovskites wherein the majority metal has partially filled d-orbitals and prove that unanticipated structures can arise when cation combinations are chosen such that very specific cation size and valence constraints are met. In both cases, the size of calcium relative to ruthenium is a critical structure-determining factor. Calcium is large enough to foster cation ordering with ruthenium yet small enough to fit into the octahedral B-site of perovskite. The scarcity of other cation-substituted compositions at either ambient or high pressure underscores the strict size and valence requirements that must be met by the constituent cations to achieve 1:2 B-site-ordered perovskite ruthenates.

Acknowledgment. The authors gratefully acknowledge funding from the National Science Foundation, Solid State Chemistry (Award DMR-9727516), and made use of the Central Facilities supported by the MRSEC program of the NSF (Grant DMR-0076097) at the Materials Research Center of Northwestern University. The work at IPNS was supported by DOE W-31-109-ENG-38. J.T.R. was supported by a National Science Foundation graduate research fellowship. J.T.R. thanks the 2000 Summer Program in Japan supported by Monbusho and NSF. The TEM work at the CRISMAT laboratory was supported by the Basse Normandie Region in the frame of the collaboration with Northwestern University.

JA044797W

(27) Battle, P. D.; Jones, C. W. *J. Solid State Chem.* **1989**, *78*, 108.
(28) Dussarrat, C.; Fompeyrine, J.; Darriet, J. *Eur. J. Solid State Inorg. Chem.* **1995**, *32*, 3.
(29) Galasso, F.; Pyle, J. *J. Phys. Chem.* **1963**, *67*, 1561.
(30) Attfield, J. P. *Int. J. Inorg. Mater.* **2001**, *3*, 1147.